

# The Effect of Granulated Fe Cluster-doped CNTs Support on The Catalytic Performance of NiO Catalyst in the DRM Reaction

*E. Kutelia*<sup>1,\*</sup>, *K. Dossumov*<sup>2</sup>, *G. Yergazyeva*<sup>2</sup>, *D. Gventsadze*<sup>1</sup>, *N. Jalabadze*<sup>1</sup>, *T. Dzigrashvili*<sup>1</sup>, *L. Nadaraia*<sup>1</sup>, *O. Tsurtsunia*<sup>1</sup>, *M. Mambetova*<sup>2</sup>

This study first demonstrated the possibility of the production of catalyst supports in the form of granules and tablets composed of nanoparticles of Fe atom cluster-doped CNTs using mini-mold forming and spark plasma sintering (SPS) techniques respectively. The pilot samples of the novel catalyst system containing 3% NiO active phase, synthesized on the granulated Fe cluster-doped CNTs carrier, were tested to determine their catalytic activity and coking resistance in the DRM reaction, in a wide range of temperatures up to 900°C. The developed novel catalyst systems' samples were characterized before and after the catalyst reaction using SEM, EDX, XRD, and AES methods. It is shown that the temperature dependence of the catalytic activity of the 3% NiO catalyst, supported on the granulated Fe cluster-doped CNTs carrier, revealed two characteristic temperature ranges with different rates of efficiency. Particularly, at high reaction temperatures, starting from 700°C, the conversion rates of methane and carbon dioxide (42.4% and 45.6% respectively) have more than doubled at 850°C. Starting from 850°C to 900°C the latter tends to exceed the carbon dioxide conversion rate, and at 900°C it amounts to 95%.

## Introduction

Dry reforming of methane (DRM) considerably reduces greenhouse gas emissions by converting CO<sub>2</sub> and CH<sub>4</sub> into syngas. The development of an environmentally safe industrial technology for the production of synthesis gas from methane in the presence of carbon dioxide is directly linked to the development of cost-effective catalyst systems (catalyst + carrier/support) with good catalytic performance, high resistance to carbon/coke formation, and high-temperature stability in the DRM reaction. The relevant reviews of the last decade's literature [1-5] lead to the conclusion that nickel oxide, along with other 3d-elements' oxides, appears to be one of the most forward-looking basic supported catalyst materials as an efficient substitute to the precious (Pd, Pt, Ru, etc.) metal-based catalysts. The matter is that the nickel-based catalyst system with the granulated carriers is predominantly used in the dry reforming reaction since it is more practical and economically viable compared to the noble metals-based catalyst systems. However, the primary drawback of

Ni/NiO-based catalysts is related to carbon/coke formation and the sintering of Ni particles leading to rapid deactivation of the catalyst. The recent reviews [3-5] and the research papers [6-12] clearly show that the Ni/NiO-based catalyst systems with the most frequently used synthetic and natural carriers, such as Al<sub>2</sub>O<sub>3</sub>, SiO<sub>2</sub>, zeolites, carbon materials, and other ceramic oxides, are characterized by the three more or less pronounced deficiencies in the DRM reaction: carbon/coke formation, sintering of Ni particles, and strong interaction between the support material and the active phase. It is also found that the catalytic activity of the above catalysts is significantly influenced by the nature of the support material. There are various strategies to inhibit sintering and carbon/coke formation. One of the methods is a proper selection of support materials and the development of the granulated carrier's preparation technology for the manufacturing of efficient catalyst systems with Ni/NiO active phase. From this point of view, different carbon materials, especially their nanoforms such as carbon nanotubes (CNTs) and carbon nanowires (CNWs) have recently gained a continuously growing interest in a series of applications due to their unique properties. In particular, the thermal stability, high corrosion resistance, high specific surface area, and nano/meso-sized pore structure are thought to be interesting in terms of heterogeneous catalysis and electrocatalysis as a catalyst supporter (carrier) or as a catalyst itself [13-16]. However, only scarce studies are

<sup>1</sup>Georgian Technical University, Tbilisi, Georgia

<sup>2</sup>Institute of Combustion Problems, Almaty, Kazakhstan

\*Corresponding author:

E-mail: ekutelia@gtu.ge (E. Kutelia)

available in the direction of the application of carbon nanoforms doped with 3d metals' clusters [17,18], namely Fe atom cluster-doped CNTs [19], as the granulated carriers for various catalyst systems used in the DRM reaction. This is conditioned by the obstacles in the production of catalyst carriers in the form of granules (with suitable mechanical properties) from the nanopowder composed of Fe-atom cluster-doped CNTs nanoparticles using conventional methods of granulation. In this context, the purpose of the proposed work was to demonstrate, for the first time, the possibility of preparing the granulated Fe atom cluster-doped CNTs carrier-based catalyst system with NiO active phase and investigate its catalytic activity in the DRM reaction temperature range  $500 \div 850^{\circ}\text{C}$ . The samples containing the 3% NiO active phase of the developed catalyst system were also studied by SEM, EDX, XRD, and AES methods before and after catalytic reactions to determine the carbon/coke formation process.

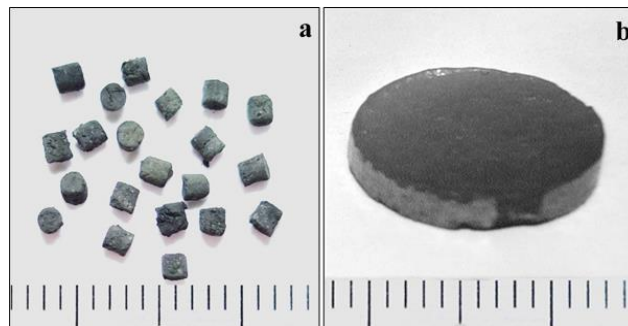
## Experimental

According to the aim of this research, for the preparation of a NiO-based catalyst system with the granulated Fe atom cluster-doped CNTs carrier, a sufficient amount of nanopowder of Fe atom cluster-doped CNTs has been synthesized using the experimental set-up providing the realization of the mechanism of doping of single CNTs with Fe atom clusters [19].

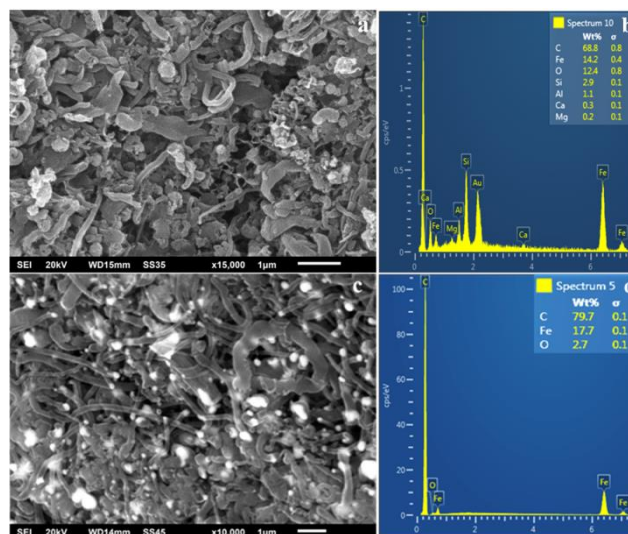
The manufacturing of granulated carrier from the above nanopowder was conducted by the following technological route: preparation of a wet mixture of Fe atom cluster-doped CNTs nanopowder + ultradispersed milled bentonite powder as a binder (up to 10%) → granulation of the obtained wet mixture using mini-mold forming → annealing during granulation and sintering simultaneous processes. The experimentally determined sintering temperature of  $550^{\circ}\text{C}/1\text{h}$  and the content of binder material ( $5 \div 10\%$ ) provide sufficient mechanical strength of the obtained granules for the preparation of the NiO-based catalyst system for the DRM reaction. Preparation of the bulk reference catalyst carrier in the form of tablets directly from the Fe atom cluster-doped CNTs nanopowder without the binder was realized using a spark plasma sintering (SPS) of the nanopowder pressed in the mold under  $\sim 20\text{ MPa}$  and heated at  $500^{\circ}\text{C}$ .

Fig. 1 demonstrates the photographic images of the granules of the catalyst carrier prepared from the mixture (Fe atom cluster-dop. CNTs nanopowder + 10% of bentonite ultradispersed powder) via the mini-mold forming method (a) and the tablet carrier prepared from pure Fe atom cluster-dop. CNTs nanopowder via SPS technique (b). The SEM images and the respective EDX spectra of the catalyst carriers' surfaces demonstrated in Fig. 1(a) and Fig. 1(b), are shown in Fig. 2(a,b) and Fig. 2(c,d) respectively. As seen from these figures, the support material tableted via SPS is of higher density and has stronger bonds between the CNT nanoparticles than

that of granulated, produced via mini-mold forming. However, here should be noted that the manufacturing of catalyst supports using the SPS technique is a complex and low-productive process for the mass production of granulated catalyst supports.



**Fig. 1.** Photographic images of the granules of catalyst carrier prepared from the mixture Fe atom cluster-doped CNTs nanopowders +10% milled bentonite ultra-dispersive powder via the mini-mold forming method (a) and the tableted carrier prepared from pure Fe atom cluster-doped CNTs nanopowder using SPS technique (b).



**Fig. 2.** SEM images and the respective EDX spectra of the surfaces of the catalyst carrier material's samples (shown in Fig. 1. a and b) manufactured from the Fe-atom cluster-doped CNTs nanopowder (with the addition of 10% Bentonite as a binder) using a mini-mold forming method of granulation (a, b) and the SPS technique for tableting of the same nanopowder without binder (c, d).

That is why for the further manufacturing and study of the NiO catalyst-based new catalyst system's carrier material with Fe atom cluster-doped CNTs, we used the granulated carriers obtained via mini-mold forming. The above synthetic nanocomposite granulated carrier-based catalyst system with  $\sim 3\text{wt}\%$  NiO active phase was prepared via impregnation of the granules according to their moisture capacity with the aqueous solution of  $\text{Ni}(\text{NO}_3)_2 \cdot 6\text{H}_2\text{O}$  as a nickel precursor. The obtained catalyst system samples after drying at  $300^{\circ}\text{C}/2\text{h}$  and subsequent calcination at  $500^{\circ}\text{C}/3\text{h}$  have been tested on catalytic activity in the

reaction of carbon dioxide conversion of methane in a wide range of temperatures up to 900°C.

The catalytic activity was evaluated on the flow-through laboratory setup following the method described previously in [11].

The process conditions: 0.1 MPa, Temperature was set in the range of 500-850°C, the ratio of methane/carbon dioxide 1:1, the volume of catalyst in the reactor 2ml, weight hour space velocity  $W=1000h^{-1}$ , feed gas velocity  $V_{fg} = 33.3ml/min$ . The samples of the developed granulated Fe atom cluster-doped CNTs carrier-based catalyst system with the 3% NiO active phase were also studied before and after catalytic reaction in a comprehensive manner using SEM/EDX (JSM 6510 LV, JEOL, Japan), AES (LAS-2000, Riber, France) and XRD (HZG-4, Germany) methods.

## Results and discussion

**Fig. 3** presents the  $CH_4$  and  $CO_2$  conversions, as well as the  $H_2/CO$  ratio obtained during the DRM experiments in the presence of the 3% NiO-based catalyst system with the granulated Fe atom cluster-doped CNTs nanopowder carrier with 10% of ultradispersed bentonite as a binder.

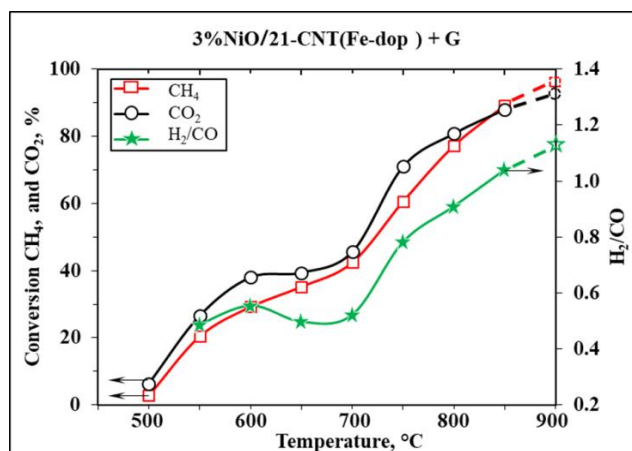


**Fig. 3.** Temperature dependence of the catalytic activity of 3%NiO-based catalyst system with granulated Fe cluster-doped CNTs nanopowder carrier containing 10% ultra-dispersive bentonite as a binder.

The temperature dependence of the catalytic activity of the 3%NiO catalyst, supported by the developed granulated carrier which has not been used previously as catalyst support for the carbon dioxide conversion of methane, revealed two characteristic temperature ranges with the different rates of efficiency of the investigated catalyst system. Particularly, at high reaction temperatures, starting from 700°C, the conversion rates of methane and carbon dioxide (42.4% and 45.6% respectively) have more than doubled at 850°C while in the low-temperature range of 550-700°C the growth in the activation rates in dependence on temperature increase is weaker. It should be pointed out that in the whole temperature range of 500-800°C the conversion rate of carbon dioxide is higher than that of

methane. However, starting from 850°C to 900°C the latter tends to exceed the carbon dioxide conversion rate, and at 900°C it amounts to 95%.

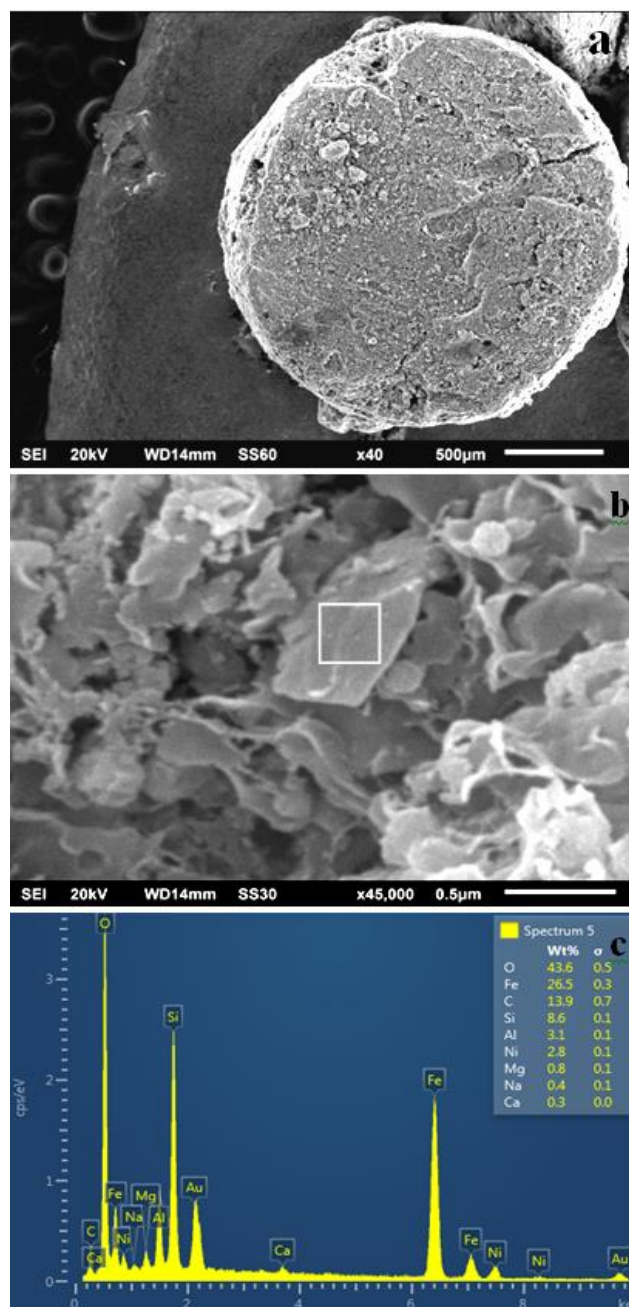


**Fig. 4.** SEM images (a, b) and the respective EDX spectra (c) taken from the surface of the selected area of the 3%NiO-based catalyst system sample with the Fe cluster-doped CNTs granulated carrier containing ultra-dispersive bentonite as a binder **before** the DRM reaction.

A comprehensive study of the samples of the developed catalyst system before and after catalytic reaction tests was performed using SEM, EDX, XRD, and AES methods to detect carbon/coke formation on the surface of the catalyst and phase transformations of the catalyst in the reaction medium of the DRM process. **Fig. 4**

and Fig. 5 demonstrate the results of SEM and EDX analyses respectively, conducted before and after the DRM reaction of the 3% NiO-base catalyst system's samples with the Fe atom cluster-doped CNTs granulated carrier containing the ultradispersed bentonite as a binder. The SEM images confirm that the distribution of bentonite ultradispersed particles as the binder and the majority of the CNTs nanopowder particles is uniform within the volumes of the granules (see Fig. 4(b) and Fig. 5(b)). In addition, the analyses of the respective EDX spectra taken from the selected local areas of the binder particles (Fig. 4(c)) as well as from the Fe cluster-doped CNTs nanoparticles (Fig. 5(c)), show that their surfaces are coated with the very thin nano-grained layer of NiO catalyst. The thickness of the NiO catalyst layer does not exceed some hundred Angstroms as testified by the fact that the EDX spectrum induced by a 20KeV energy electron beam, in addition to the peaks corresponding to Ni atoms, the peaks of the atoms contained in the carrier material (Fe cluster-dop.CNT + bentonite) are also present, including the peaks caused by the carbon atoms adsorbed from the atmosphere in the case of the samples tested before reaction (Fig. 4(c)). The carbon peak intensity of the latter, recorded from some samples of the bentonite particle surfaces after the DRM reaction, is increased to some extent. This is, obviously, related to the formation of free carbon in the form of an amorphous film on the surface of the catalyst during the DRM reaction. Here should be noted that, as it is clear from Fig. 5(b), in the considered case of free carbon formation on the catalyst's surface, precipitation of free carbon on the catalyst surface was not performed via the formation of MWCNTs or CNFs. It is apparent that in the process of the DRM reaction the formation of the free carbon nano-layer in the form of carbon gum occurs simultaneously on the surfaces of NiO catalyst coated on the particles of the carrier's components, Fe cluster-doped CNTs, and bentonite. However, it is impossible to detect and identify the EDX peaks of the free carbon modification precipitated on the surface of the catalyst formed on CNTs, separately from that of the CNTs EDX spectrum.

The XRD study of the same granulated Fe atom cluster-doped CNTs carrier-based catalyst system's samples with the 3%NiO active phase before and after the DRM reaction has been carried out using the X-ray diffractometer at 40KeV and 30mA with the CuK $\alpha$  radiation and Ni filter in the range of 20-80° of 2 $\theta$  values. Fig. 6 displays the respective XRD patterns of the above catalyst system's samples recorded before (pattern 1) and after (pattern 2) the DRM reaction tests. The X-ray diffraction pattern, taken from the sample before the reaction test (pattern 1), shows only a full set of peaks corresponding to Fe<sub>2</sub>O<sub>3</sub> while the peaks of NiO catalyst, synthesized on the surface of the carrier by wet impregnation and subsequent drying and calcination at the respective temperatures, are absent. As a result, no obvious peaks corresponding to NiO have been observed that could be attributed to their ultra-fine-grained (<100Å) "X-ray

amorphous" form deposited on the carrier's surface as well as to their modest amount (~3%) in contrast to the carrier material. The latter is in accordance with our estimates of their thickness (<1000Å) based on the SEM-EDX analysis.

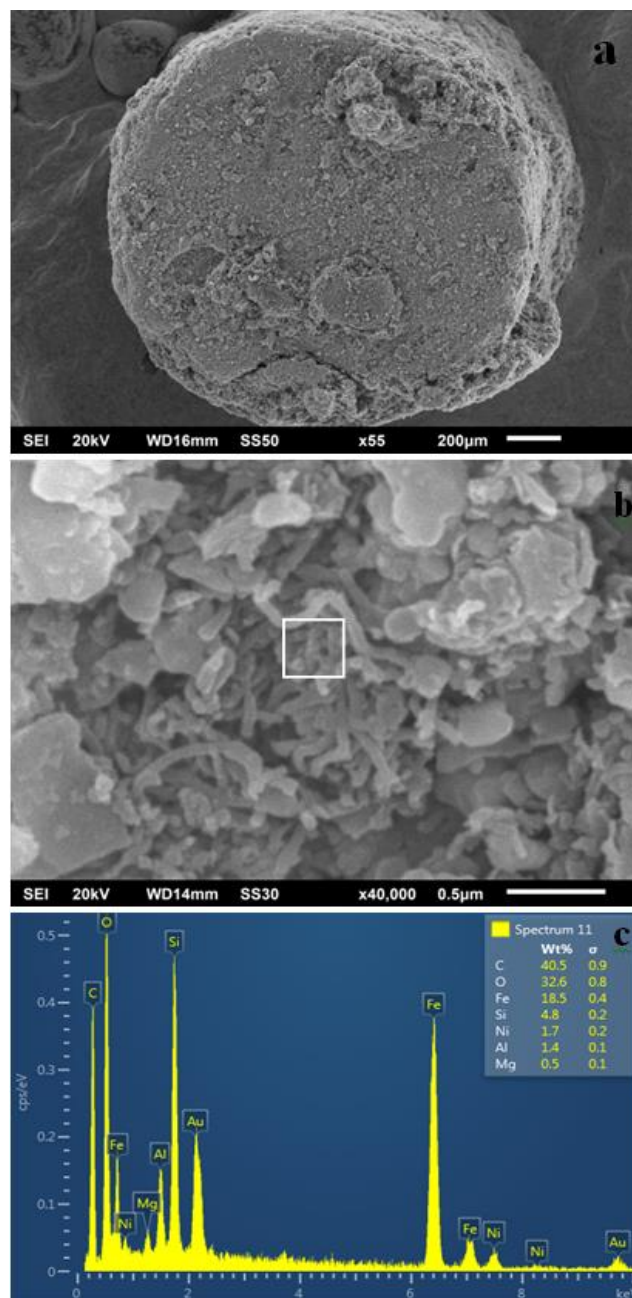
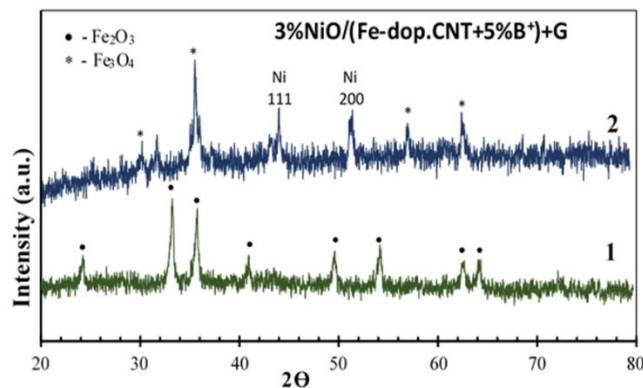


Fig. 5. SEM images(a, b) and the respective EDX spectra (c) taken from the surface of the selected area of the 3%NiO-based catalyst system sample with the Fe cluster-doped CNTs granulated carrier containing ultra-dispersive bentonite as binder after the DRM reaction.

It is evident that the presence of Fe<sub>2</sub>O<sub>3</sub> is conditioned by the oxidation process of Fe atom clusters that dope each CNT nanoparticle in the carrier granules during the technological route of manufacturing the developed catalyst system.



**Fig. 6.** The XRD patterns of the samples of 3%NiO-based catalyst system with the Fe cluster-doped CNTs granulated carrier containing ultra-dispersive bentonite as binder recorded before (pattern 1) and after (pattern 2) the DRM reaction.

The XRD pattern 2 (**Fig. 6**), recorded from the sample of the same catalyst system after the DRM reaction test in the temperature range 500–850°C shows three different distinctions: the first is a set of easily distinguishable peaks at  $2\theta$  of 44.5° and 51.7° that can undoubtedly be assigned to the metallic Ni phase peaks that are typical X-ray reflections from the (111) and (200) atomic planes of a nickel crystal lattice. The latter confirms that the sintering (recrystallization) of Ni nanoparticles reduce from NiO by hydrogen, which occurred at high temperatures of the reaction. The second distinction is the presence of carbon revealed by the formation of the very low-intensity peak at  $2\theta = 26.2^\circ$  corresponding to the (0002) atomic plane of graphite or multi-layered graphene. The third is an occurrence of a full set of peaks of the  $\text{Fe}_3\text{O}_4$  phase indicating the transformation of the  $\text{Fe}_2\text{O}_3$  oxide to  $\text{Fe}_3\text{O}_4$  in the reaction medium of the DRM process.

A good correlation between the results obtained from the SEM-EDX and XRD analyses of the developed catalyst system leads to the conclusion that the considered catalyst system can suppress the free carbon/coke formation process in the wide range of temperatures of the DRM reaction. To explain the phenomenon of the suppression of free carbon formation in the forms of CNWs and MWCNTs during the DRM reaction for the above catalyst system and to determine the structural types of the surface carbon species formed at high temperatures, the sample of the developed catalyst system taken after the DRM reaction tests and the sample prepared as a reference from the pure Fe atom cluster-doped CNTs nanopowder tableted via SPS (**Fig. 1(b)**) were additionally tested using an AES technique.

**Fig. 7** demonstrates the differential Auger-electron spectra recorded in the 200–600 eV energy range from the surface of the tablet carrier prepared from pure Fe atom cluster-doped CNTs nanopowder via SPS technique (**a**) and the surface of the NiO catalyst synthesized on the granulated mixture (Fe atom cluster-doped CNTs nanopowder +10% of ultradispersed bentonite powder) carrier prepared via mini-mold forming after the DRM

reaction at 850°C (**b**). Both spectra are recorded after the removal of a  $\sim 100\text{\AA}$  thickness layer (including the physically adsorbed from the atmosphere  $\sim 30\text{\AA}$  thickness nanolayer which exists at the top of any solid loaded from the air) via bombardment by 2KeV energy argon ions in the analytical chamber of the Auger spectrometer.

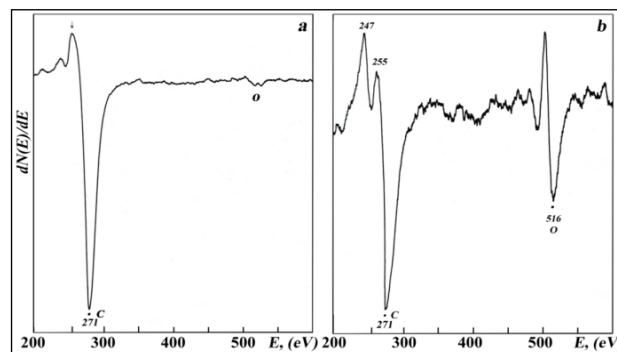


**Fig. 7.** Differential Auger-electron spectra, recorded from the surface of tablet carrier prepared from the pure Fe-atom cluster-doped CNTs carrier nanopowder via SPS technique (a) and the surface of 3%NiO-based catalyst system with granulated Fe cluster-doped CNTs nanopowder carrier containing 10% ultra-dispersive bentonite as binder after the DRM reaction test (b). Both spectra were recorded after sputtering of a  $\sim 100\text{\AA}$  thickness surface layer via bombardment by 2KeV energy argon ions.

Based on the composition of the tableted carrier shown in **Fig. 7(a)**, the differential Auger spectrum (peak at 271 eV corresponding to carbon atoms' KLL Auger-electron transition) may be regarded as a reference Auger spectrum of the Fe atom cluster-doped CNTs. In addition, the negligibly small peak at 510 eV corresponding to the oxygen atoms'  $\text{KL}_{23}\text{L}_{23}$  Auger-electron transition confirms that Fe atoms in the doping CNT clusters are not oxidated. Obviously, in the case of free carbon formation in the form of MWCNTs (or CNWs) on the surface of the NiO catalyst system during the DRM reaction, the same carbon atoms' KLL Auger-transition peak, as in **Fig 7(b)**, should occur. However, the differential Auger-spectrum (**Fig.7(b)**) recorded from the surface of the NiO-based catalyst system's sample after the DRM reaction test, clearly shows that the carbon atoms' KLL Auger-transition peak at 271 eV changed in shape due to the appearance of plasmon peaks on the side of the fewer energies (274 eV and 255 eV). Moreover, a significant increase in the intensity of oxygen atoms' Auger-transition peak at 516 eV has been detected when compared with the spectrum shown in **Fig. 7(a)**. The latter justifies that Fe atoms are oxidated and this correlates with the XRD data. On the other hand, the determination of types of surface carbon species (pyrolytic coke, CNW, MWCNT, gum with multi-layered graphene and graphite), in contrast to EDX spectra, is possible using the existed method of the analysis of carbon KLL Auger peaks' fine structure [20]. The comparative study of the fine structure of carbon atoms' KLL Auger-transition peaks in the differential Auger-electron spectra recorded from the 3% NiO-based catalyst systems with the granulated CNTs

nanopowder (containing the bentonite binder) carrier and the existed different synthetic and natural raw materials-based granulated carriers [12] lead to the conclusion that after the DRM reaction at high temperature short-range ordered free carbon deposits are formed on the surfaces of the developed catalyst system. These deposits can exist in the form of carbon atom groups distinguished in  $sp^3$  or ( $sp^2 + sp^3$ ) mixture of electronic hybridization with the different ratios between the carbon  $C\alpha$  and  $C\gamma$  phases in the polymerized gum-like nanofilm ( $\leq 1000\text{\AA}$ ), depending on the reaction temperature.

A good correlation between the obtained SEM-EDX, XRD, and AES results regarding the structural transformations in the novel Fe atom cluster-doped CNTs nanopowder granulated carrier-based catalyst system with the 3% NiO active phase allows concluding that the revealed peculiarities of catalytic activity of the developed catalyst system in the wide range of DRM reaction temperatures (up to  $900^\circ\text{C}$ ), and the suppression of the free carbon formation process in the form of MWCNTs and CNWs at high reaction temperatures is a result of a superposition (assemble effect) of the intrinsic catalytic activity of the nano-compositional carrier as a co-catalyst and the ultra-fine-grained NiO active phase's catalytic performance.

## Conclusion

This study demonstrates, for the first time, the possibility of catalyst carriers' production in the form of granules (or tablets) with suitable mechanical properties, that are composed of nanoparticles of Fe cluster-doped CNTs, using two different methods of preparation: mini-mold forming and spark plasma sintering. The novel catalyst system containing a 3% NiO active phase, synthesized on the surface of the granulated Fe cluster-doped CNTs carrier, was prepared by a capillary impregnation technique and tested to determine its catalytic activity and coking resistance in the DRM reaction. A comprehensive study of the samples of the developed catalyst system before and after catalytic reactions was performed using SEM, EDX, XRD, and AES methods to determine the carbon/coke formation processes.

It is shown that the catalytic activity of the 3% NiO catalyst, supported on the granulated Fe cluster-doped CNTs carrier, which has not been used previously as catalyst support for carbon dioxide conversion of methane, revealed two characteristic temperature ranges with different rates of efficiency. Particularly, at high reaction temperatures, starting from  $700^\circ\text{C}$ , the conversion rates of methane and carbon dioxide (42.4% and 45.6% respectively) have more than doubled at  $850^\circ\text{C}$  while in the low-temperature range of  $550\text{--}700^\circ\text{C}$  the growth in the activation rates in dependence on temperature increase is weaker. Starting from  $850^\circ\text{C}$  to  $900^\circ\text{C}$  the latter tends to exceed the carbon dioxide conversion rate, and at  $900^\circ\text{C}$  it amounts to 95%.

The authors propose that the revealed peculiarities in the catalytic activity of the developed NiO-based catalyst system with the Fe cluster-doped CNTs granulated carrier in the wide range of DRM reaction temperatures, and the suppression of the free carbon formation process in the forms of MWCNTs and CNWs at high reaction temperatures, are the results of a superposition of the intrinsic catalytic activity of the nano-compositional support as a co-catalyst and the catalytic performance of ultra-fine-grained NiO active phase.

## Acknowledgments

This work has been performed with the financial assistance of the International Science and Technology Center within the project GE-2606.

## Conflicts of interest

Please ensure that a conflict of interest statement is included in your manuscript here. Please note that this statement is required for all submitted manuscripts. If no conflicts exist, please state that "There are no conflicts to declare".

## Keywords

Catalytic system, Fe cluster-doped CNTs, granulated carrier, DRM, Nickel oxide

## References

1. Guojie Zhang, Jiwei Liu, Ying Xu Yingshiu Sun.; *International Journal of Hydrogen Energy*, **2018**, *43*, 15030. DOI: <https://doi.org/10.1016/j.ijhydene.2018.06.091>
2. Nicolas Abdel Karim Aramouni; Jad G. Touma; Belal Abu Tarboush; *Renewable and Sustainable Energy Review*, **2018**, *82*, 2570. DOI: <https://doi.org/10.1016/j.rser.2017.09.076>
3. Luqmanulhakim Baharudin; Norhasyimi Rahmat; Nur Hidayati Othman; Nilay Shah; Seyd Shatir A. Seyd-Hassan.; *Journal of CO2 Utilization*, **2022**, *61*, 102050. <https://doi.org/10.1016/j.jcou.2022.102050>
4. Abdulrahman Abdulrasheed, Aishah Abdul Jalil, Yahya Gambo, Maryam Ibrahim, Hambali Umar Hambali, Muhamed Yusuf Shahul Hamid.; *Renewable and Sustainable Energy Review*, **2019**, *108*, 175. DOI: <https://doi.org/10.1016/j.rser.2019.03.054>
5. Aziz, M.A.A.; Setiabudi, H.D.; The, L.P.; Annuar, N.H.R.; Jalil, A.A.; *Journal of the Taiwan Institute of Chemical Engineering*, **2019**, *101*, 139. DOI: <https://doi.org/10.1016/j.jtice.2019.04.047>
6. Karam Jabbour, Nissirine El Hassan, Davidson, A.; Massiani, P.; Casale, S.; *Chemical Engineering Journal*, **2015**, *264*, 351. DOI: <https://doi.org/10.1016/j.cej.2014.11.109>
7. Frontera, P.; Macario, A.; Aloise, A.; Antonucci, P.L.; Giordano, G.; Nagy, J.B.; *Catalysis Today*, **2013**, *218*, 18. DOI: <https://doi.org/10.1016/j.cattod.2013.04.029>
8. Subhasis Das, Sharvani Thakur, Arijit Bag, Manveer Singh Gupta, Prasenjit Mondal, Ankur Bordoloi.; *Journal of Catalysis*, **2015**, *330*, 60. DOI: <https://doi.org/10.1016/j.jcat.2015.06.010>
9. Anis H. Fakeeha, Wasim U. Khan, Ahmed S. Al-Fatesh, Ahmed E. Abasaed.; *Chinese Journal of Catalysis*, **2013**, *34*, 764. DOI: [https://doi.org/10.1016/S1872-2067\(12\)60554-3](https://doi.org/10.1016/S1872-2067(12)60554-3)
10. Hongrui Liu, Haithem Bel Hadj Taief, Mourad Benzina.; *Catalysis Today*, **2018**, *306*, 51. DOI: <https://doi.org/10.1016/j.cattod.2016.12.017>
11. Kutelia, E.R.; Dossuomov, K.D.; Gventsadze, D.I.; Yergaziyeva, G.E.; Dzigrashvili, T.A.; Mambetova, M.M.; Jalabadze, N.V.; Myltykbaeva, L.K.; Nadaraia, L.V.; Tsurtsunia, O.O.; Gventsadze, L.D.; Kukava, T.G.; Telbayeva, M.M.; *Georgian Engineering News*, **2021**, *2*, 56.
12. Kutelia, E.; Dossuomov, K.; Mambetova, M.; Dzigrashvili, T.; Eristavi, B.; Nadaraia, L.; Jalabadze, N.; Gventsadze, D.; Tsurtsunia, O.; Yergaziyeva, G.; Myltykbaeva, L.; Kukava, T.;

- Gventsadze, L.; Telbayeva, M; *American Institute of Physics*, **2022**, in publication
13. Yong-Ming Dai, Chi-Yuan Lu, Chi-Jen Chang.; *RSC Advances*, **2016**, 6, 73887.
  14. Basri, S.; Kamarudin, S.K.; Daud, W.R.W.; Yaakub, Z.; *International Journal of Hydrogen Energy*, **2010**, 35, 7957.  
**DOI:** <https://doi.org/10.1016/j.ijhydene.2010.05.111>
  15. Calvillo, L.; Celorrio, V.; Moliner, R.; Garcia, A.B.; Camean, I.; Lazaro, M.J.; *Electrochimica Acta*, **2013**, 102, 19.  
**DOI:** <https://doi.org/10.1016/j.electacta.2013.03.192>
  16. Mehrmoush Khavarian, Siang-Piao Chai, Abdul Rahman Mohamed; *Chemical Engineering Journal*, **2014**, 257, 200.  
**DOI:** <https://doi.org/10.1016/j.cej.2014.05.079>
  17. Kvande, I.; Yu, Z.; Zhao, T.; Ronning, M.; Holmen, A.; Chen, D.; *Chemistry for Sustainable Development*, **2006**, 14, 583.
  18. Faramarz Sadeghzadeh-Darabi, Mohsen Padervand, Mohammad Khodadadi-Moghaddam, Hadi Salari, SeyedSaeed Ahmadvand, Mohammad Reza Gholami.; *Advanced Science, Engineering and Medicine*, **2012**, 2, 294.  
**DOI:** <https://doi.org/10.1166/asem.2012.1176>
  19. Kutelia, E.; Rukhadze, L.; Jalabadze, N.; Dzigrashvili, T.; Tsursumia, O.; Gventsadze, D.; *Advanced Materials Letters*, **2018**, 9(12), 867. **DOI:** [10.5185/amlett.2018.2144](https://doi.org/10.5185/amlett.2018.2144)
  20. Mizokava, Y.; T. Miysato, T.; S. Nakamura, K.M. Geib, C.W. Wilmsen.; *Surf. Sci.*, **1987**, 182, 431.  
**DOI:** [10.1016/0039-6028\(87\)90011-2](https://doi.org/10.1016/0039-6028(87)90011-2)